AGU100 ADVANCING EARTH AND SPACE SCIENCE

JGR

Journal of Geophysical Research: Atmospheres

RESEARCH ARTICLE
10.1029/2018JD028412

Key Points:
- This work represents the first modeling study of long-term trend in gas-phase ammonia concentration ($[NH_3]$) over the United States
- Model simulations, consistent with observations, show increase in $[NH_3]$ over the United States, with magnitude of relative change largest in the East and smallest in the West
- Decreasing SO_2 and NO_x emissions respectively contribute to 2/3 and 1/3 of the increase in $[NH_3]$ over the United States

Supporting Information:
- Supporting Information S1

Correspondence to:
F. Yu,
fyu@albany.edu

Citation:
Yu, F., Nair, A. A., & Luo, G. (2018). Long-term trend of gaseous ammonia over the United States: Modeling and comparison with observations. *Journal of Geophysical Research: Atmospheres*, *123*, 8315–8325. https://doi.org/10.1029/2018JD028412

Received 28 JAN 2018
Accepted 22 JUN 2018
Accepted article online 6 JUL 2018
Published online 12 AUG 2018

Long-Term Trend of Gaseous Ammonia Over the United States: Modeling and Comparison With Observations

Fangqun Yu[1], **Arshad Arjunan Nair**[1], **and Gan Luo**[1]

[1]Atmospheric Sciences Research Center, State University of New York at Albany, Albany, NY, USA

Abstract The concentrations of atmospheric ammonia ($[NH_3]$) have been observed to be increasing over the United States in the last decade, especially in Eastern United States. It is important to understand this temporal trend and variation due to the role of NH_3 in particle formation and its ecological effects. Here the long-term trend of $[NH_3]$ over the United States is investigated using GEOS-Chem, a global 3-D tropospheric chemistry model, and is corroborated with empirical evidence from the Ammonia Monitoring Network. Model simulations, consistent with observations, show increase in $[NH_3]$ over the United States from 2001 to 2016, with magnitude largest in the East (~5% to 12%/year) and smallest in the West (~0% to 5%/year). Reasons for this are examined, and evidence for the role of decreasing SO_2 and NO_x emissions in increasing $[NH_3]$ is provided. The contributions of meteorology and NH_3 emission changes to the $[NH_3]$ increase appear to be small during the period. Our sensitivity study suggests that decreasing SO_2 and NO_x emissions over the United States owing to stringent regulations explain about 2/3 and 1/3 of the increase in $[NH_3]$, respectively. This effect is different for various NH_3 and SO_2 and NO_x regimes. Given the continued reduction of SO_2 and NO_x emissions due to U.S. regulations mainly aimed at $PM_{2.5}$ reduction, the present results are important towards better assessing the environmental impact of emission controlling policies.

1. Introduction

Ammonia (NH_3) is the primary alkaline gas in the atmosphere largely from agricultural activities and is well known to play a significant role in the formation of $PM_{2.5}$ by the neutralization of acidic species resulting from SO_2 and NO_x in the atmosphere. In addition, ammonia deposition can lead to negative ecosystem effects such as acidification and eutrophication (Erisman et al., 2007; Fangmeier et al., 1994), especially in sensitive ecosystems such as alpine terrain and wetlands (Beem et al., 2010; Ellis et al., 2013). Recently, ammonia has been receiving additional attention because of its potential to enhance new particle formation in the atmosphere (Kirkby et al., 2011) and thus affect particle number abundance, which is important for aerosol indirect radiative forcing. While emission controlling policies aimed to improve air quality have led to substantial SO_2 emission reductions and limited NO_x emission reductions in Europe and North America, NH_3 emissions have seen no or much smaller reductions in these regions (European Environment Agency, 2017). It is important to understand the variations of ammonia concentration ($[NH_3]$) in the atmosphere, its response to SO_2 and NO_x emission reductions as well as climate change, and its long-term trend.

There have been a number of studies, especially in the recent years, that examine the long-term trend of $[NH_3]$. Most of these studies have been based on long-term surface-based observations (Alebic-Juretic, 2008; Ferm & Hellsten, 2012; Horvath et al., 2009; Hu et al., 2014; Li et al., 2017; Schiferl et al., 2016; Tang et al., 2009, 2018; Wichink Kruit et al., 2017; Yao & Zhang, 2016; van Zanten et al., 2017), although inferences of long-term $[NH_3]$ trend have also been made recently using remote sensing (Schiferl et al., 2016; van Damme et al., 2014; Warner et al., 2017). A common theme to these observations is that the trend of $[NH_3]$ generally does not follow the trend in its emission, which is generally reducing or does not change. Most long-term records of surface $[NH_3]$ measurements are available for Europe and a number of studies indicate that $[NH_3]$ does not see a corresponding decreasing trend as ammonia emissions (Alebic-Juretic, 2008; Ferm & Hellsten, 2012; Horvath et al., 2009; Tang et al., 2009, 2018; van Zanten et al., 2017; Wichink Kruit et al., 2017). For example, Horvath et al. (2009) showed the 25-year long-term $[NH_3]$ in Hungary did not decrease even in the period of large ammonia emission reduction. Ferm and Hellsten (2012) observed a significant decrease for particulate ammonium and an increase in gaseous ammonia at four remote mountainous sites in Sweden from

1986 to 2010. Over North America, analysis of available [NH_3] data generally indicates either no significant change or an increasing trend (Hu et al., 2014; Li et al., 2017; Schiferl et al., 2016; Yao & Zhang, 2016). For example, analysis of the Ammonia Monitoring Network (AMoN) data from 2008 to 2015 by Butler et al. (2016) indicates the concentrations of NH_3 have been increasing across United States despite the nearly constant emissions during this period. On a global scale, Warner et al. (2017) found, based on analysis of a 14-year (2003–2016) AIRS satellite record, increasing [NH_3] trends over the major agricultural areas in the United States (2.61%/year), the European Union (EU; 1.83%/year), and China (2.27%/year). The possible reasons behind the observed long-term trends, as pointed out in various data analysis studies, include changes in NH_3 emissions, anthropogenic SO_2 and NO_x emissions, and ammonia phase partitioning, and meteorology (Sutton et al., 2003).

In contrast to a large number of [NH_3] long-term trends data analysis papers mentioned above, we found in the literature only two modeling studies on long-term trends of [NH_3] (Horvath et al., 2009; Wichink Kruit et al., 2017), both focusing on limited areas in Europe (one in Hungary for the period of 1989–2004 using the European Monitoring and Evaluation Programme model and the other in the Netherlands for the period of 1993–2014 based on the Operational Priority Substances model). In the present study, we examine the long-term trend in [NH_3] in the United States using a 3-D global tropospheric chemistry model (GEOS-Chem; e.g., Bey et al., 2001). The simulated [NH_3] values and trends are compared with those observed from a surface ammonia monitoring network, and the extent of the contribution of SO_2 and NO_x emission changes to the long-term [NH_3] trends is determined by considering various emission scenarios. To our knowledge, modeling studies focusing on long-term trends of [NH_3] in the United States have not been reported prior to this study.

2. Methods

2.1. Model and Simulations

The modeling work in this study is based on the GEOS-Chem model with the Advanced Particle Microphysics (APM) model incorporated (Yu & Luo, 2009). GEOS-Chem is a global 3-D model of atmospheric composition driven by assimilated meteorological observations from the Goddard Earth Observing System (GEOS) of the NASA Global Modeling and Assimilation Office (GMAO). The model has been developed and used by many research groups and contains a number of state-of-the-art modules treating emissions (Keller et al., 2014; van Donkelaar et al., 2008), and various chemical and aerosol processes (e.g., Bey et al., 2001; Evans & Jacob, 2005; Martin et al., 2003; Murray et al., 2012; Park et al., 2004; Pye & Seinfeld, 2010). In GEOS-Chem v10-01, on which this study is based, major atmospheric components are simulated with the NO_x-O_x-hydrocarbon-aerosol chemistry (Bey et al., 2001; Martin et al., 2003). Thermodynamic equilibrium of inorganic aerosols is calculated with ISORROPIA II scheme (Fountoukis & Nenes, 2007). Formation and aging of secondary organic aerosols are based on the mechanisms developed by Pye and Seinfeld (2010) and Yu (2011). It is noteworthy that a number of previous studies have evaluated the GEOS-Chem simulation of ammonia and examined impacts of various processes on the variations of [NH_3] (Heald et al., 2012; Paulot et al., 2014; Schiferl et al., 2016; Zhang et al., 2012; Zhu et al., 2015) but none has looked into long-term trends of ammonia.

The horizontal resolution of GEOS-Chem employed for this study is 2° × 2.5° and there are 47 vertical layers (with 14 layers from surface to ~2 km above the surface). GMAO MERRA2 meteorology fields are used to drive GEOS-Chem, and simulations have been carried out for 2001–2016. Biogenic emissions and biomass burning emissions are produced by MEGAN v2.1 (Guenther et al., 2012) and GFED4 (Giglio et al., 2013), respectively. Over the United States, the focus of the present study, anthropogenic emissions are based on the Environmental Protection Agency's (EPA) National Emission Inventory (NEI) 2011. The original NEI2011 data were preprocessed with the EPA Sparse Matrix Operator Kernel Emissions (SMOKE) platform (https://www.cmascenter.org/smoke/) into GEOS-Chem emissions for 2011. The emissions processing system SMOKE is designed to create gridded hourly emissions for various atmospheric chemistry models by working with emissions inventories; temporal and chemical speciation profiles; spatial surrogates; gridded meteorology and land use data; and other ancillary files specifying the timing, location, and chemical nature of emissions. Agricultural ammonia emissions in the NEI2011 inventory are also scaled to match optimized emissions from the MASAGE_NH_3 inventory (Paulot et al., 2014).

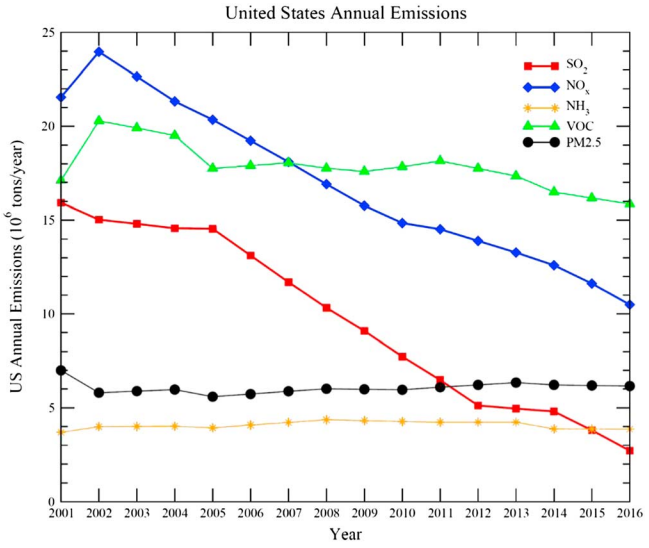

Figure 1. U.S. annual emissions of SO_2, NO_x, NH_3, anthropogenic VOC, and $PM_{2.5}$ from the U.S. Environmental Protection Agency (EPA) National Emission Inventory (NEI).

Scaling factors are generated by comparing 2005–2008 averaged MASAGE_NH_3 agricultural emissions with the NEI2011 agricultural emissions. This treatment allows the model to retain the spatial and temporal variability in NEI2011 while matching the optimized totals from MASAGE_NH_3. For multiple-year simulations presented here, Air Pollutant Emissions Trends Data from 1990 to 2016 reported by EPA (annual total emission amounts) are used to scale NEI2011 emission inventories of CO, NO, SO_2, NH_3, BC, OC, and VOCs from year 2011 to simulation year. Figure 1 shows that the U.S. anthropogenic emissions from 2001 to 2016 decreased for SO_2, NO_x, and VOC. There is a slight increase for NH_3 emission from 2001 to 2008, which came from prescribed fires, waste disposal, and municipal/commercial composting emissions. After 2008, NH_3 emission decreased slightly due to the decrease of miscellaneous emissions. The average NH_3 emission flux over North America from 2001 to 2016 is shown in Figure S1 in the supporting information.

2.2. AMoN Measurements

The AMoN provides biweekly averaged surface [NH_3] across the continental United States (National Atmospheric Deposition Program, 2017). Ammonia is passively collected by a diffusion sampler and then measured in the laboratory by sonically dislodging ammonium ions from the phosphoric acid sorbent and using flow injection analysis. There are 113 AMoN sites, but only certain sites have been operational for the long-term with the longest measurement period from November 2007 (whole month) to present. For the present analysis, a criterion we set as long-term is being operational from January 2008 or earlier till December 2016. The sites thus chosen are listed with Arabic numerals in Table 1. Sites indexed 1 to 6 are in the East, 7 to 11 in the Central region, and 12 and 13 in the West. The criterion in selection of sites is relaxed to obtain more data from the West; these sites are indexed with uppercase letters (A, B, and C). Three additional sets of sites (indexed with lowercase letters) are also chosen as they are close in location

Table 1
Selected Ammonia Monitoring Network Sites

Site index	Site ID	Lat	Lon	Elevation (m)	State	Start date	Site characteristic
1	NY67	42.40	−76.66	503	NY	10/30/2007	Agriculture
2	SC05	32.94	−79.66	1	SC	10/30/2007	Remote
3	OH02	39.31	−82.12	275	OH	10/30/2007	Remote
4	MI96	42.25	−83.20	180	MI	10/29/2007	Urban
5	OH27	39.15	−84.52	194	OH	10/30/2007	Urban
6	IN99	39.81	−86.11	230	IN	10/30/2007	Urban
7	IL11	40.05	−88.37	212	IL	10/30/2007	Agriculture
8	WI07	43.47	−88.62	287	WI	10/30/2007	Remote
9	MN18	47.95	−91.50	524	MN	10/30/2007	Remote
10	OK99	35.75	−94.67	299	OK	10/30/2007	Agriculture + Remote
11	TX43	34.88	−101.67	1,057	TX	10/30/2007	Agriculture
12	CO13	40.59	−105.14	1,570	CO	11/27/2007	Urban + Agriculture
13	NM98	36.81	−107.65	1,972	NM	01/11/2008	Remote
A	ID03	43.46	−113.56	1,807	ID	06/07/2010	Remote
B	CA83	36.49	−118.82	457	CA	03/22/2011	Remote
C	WA99	46.76	−122.12	424	WA	03/16/2011	Remote
a	OH54	39.64	−83.26	267	OH	03/01/2011	Remote
b	OH99	39.94	−81.34	371	OH	01/13/2015	Remote
c	AR09	35.62	−93.87	261	AR	10/06/2015	Remote
d	AR15	35.93	−93.85	454	AR	10/06/2015	Remote + Agriculture
e	CO88	40.28	−105.55	2,739	CO	05/10/2011	Remote
f	CO98	40.29	−105.66	3,159	CO	05/10/2011	Remote

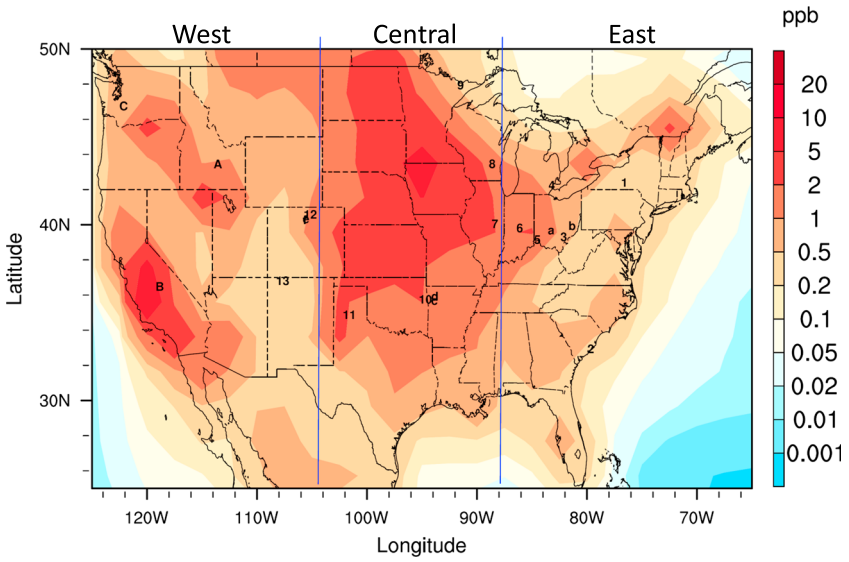

Figure 2. GEOS-Chem simulated surface layer gas-phase [NH_3] averaged from 2001 to 2016. Color bar indicates [NH_3] in ppb (parts per billion, by volume). Vertical blue line segments separate the North American region into West, Central, and East regions. The locations of AMoN sites in Table 1 are marked on the map with corresponding site index. Note that (c) and (d) (close to 10) as well as (e) and (f) (close to 12) overlap because these sites are close in location.

to the three sites (OH02, OK99, and CO13) that have long-term measurements. The motivation behind this is discussed further in text. The biweekly data are averaged (weighted with the number of days in a given month for each data point) to obtain monthly mean data. If a month is missing greater than 20 days of data, the average data for the month is omitted (~14% of times).

3. Results and Discussion

3.1. Spatial Distribution of [NH_3] Over the United States

The average surface layer simulated [NH_3] over North America from 2001 to 2016 is shown in Figure 2, with corresponding plots for [SO_2] and [NO_x] given in Figure S2. We demarcate the region as West, Central, and East due to clear spatial differences. [NH_3] is highly source dependent, that is, emissions are the main factor determining its magnitude. Figure 2 shows that regions with relatively higher ammonia surface concentrations tend to have more intensive agriculture activities (United States Department of Agriculture National Agricultural Statistics Service, 2017). The Central region, primarily over the Midwestern United States shows elevated long-term mean [NH_3], in some places >5 ppb (parts per billion, by volume). This is attributable mainly to intensive agricultural activities including fertilizer use and animal husbandry (Figure S1). The Western region shows lower average concentrations. There are however hotspots over the center of the border between Washington and Oregon as well as the Twin Falls region in Idaho. These hotspots are attributable to agricultural activities as well. Central California also shows elevated [NH_3] likely due to agriculture and biomass burning in the San Joaquin Valley. The Eastern region shows the lowest [NH_3] of the three regions, generally <2 ppb. The spatial variability of mean [NH_3] simulated by GEOS-Chem corresponded with previous model simulations (e.g., Schiferl et al., 2016) and satellite observations (Warner et al., 2016), showing highest [NH_3] in the central United States and lowest in the Eastern region.

We compare the model simulated surface [NH_3] with surface measurements by the AMoN. Figure 3 shows this for a few sites in each of the regions previously defined. In the Eastern region, a site OH02 (site index = 3) with the earliest and most continuous-to-date measurements is selected and compared with model simulated values (Figure 3a). Two other sites, OH54 and OH99, are also colocated within the model grid-box under consideration. The model captures the magnitude of [NH_3], as well as its seasonal variations, and its increasing long-term trend. The correlation coefficient (r) and mean normalized error

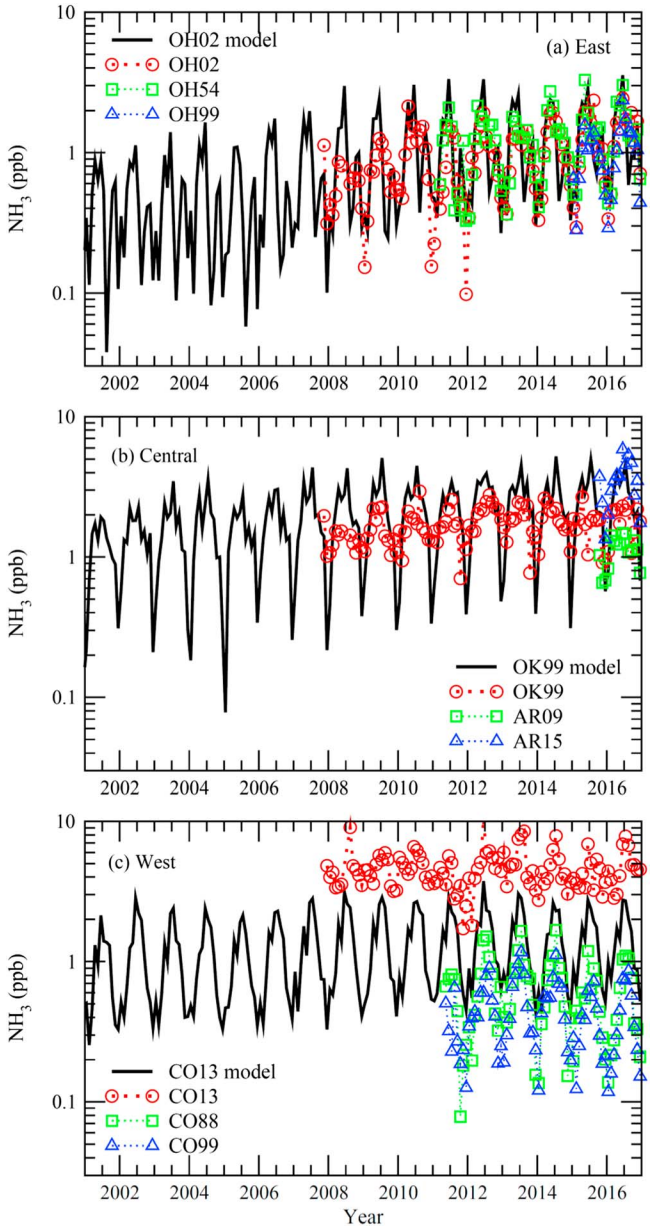

Figure 3. Modeled long-term trend of ammonia in selected sites in each region (top to bottom: East, Central, and West) denoted with solid line plot with data from colocated (within model 2° × 2.5° gridbox) AMoN sites denoted with corresponding scatter plot. The correlation coefficient (*r*) and mean normalized error (MNE) of model simulations with observations (*r*, MNE) for sites OH02, OH54, OK99, CO13, CO88, and CO99 are (0.66, 17%), (0.74, 2.7%), (0.63, 34%), (0.71, −70%), (0.85, 132%), and (0.75, 222%), respectively.

(MNE) of model simulations with observations (*r*, MNE) for sites OH02 and OH54 are (0.66, 17%) and (0.74, 2.7%), respectively. This location is remote in the Ohio River Valley, although it is near coal-powered plants and chemical plants. Regardless, the magnitude of [NH_3] is lower (<~2 ppb) than areas in the Central and Western regions. Figure 3b presents a similar analysis for a site (OK99, site index = 10) in the Central region with two other colocated sites (AR09 and AR15). The model performs reasonably well in the capture of the magnitude, temporal variations, and trend of ammonia, with r = 0.63 and MNE = 34% for site OK99. The model also captures the agricultural hotspot in the tri-junction of Oklahoma-Arkansas-Missouri. Data for AR15 are only for a year and a half; however, it shows better model-measurement correlation with regard to the magnitude and temporal variation. This is due to the site being in farmland with likely livestock farming, a better representative of the area under consideration. AR09 (remote location on a hill) has the lowest concentrations but a similar seasonal variation. For a site in the Western region (CO13, Figure 3c), the model captures the intra-annual variation with no significantly changing long-term trend; these aspects are confirmed by the surface measurements (with r = 0.71, 0.85, and 0.75 for CO13, CO98, and CO99, respectively). However, the model predicted magnitude appears to be lower (CO13, MNE = −70%) or higher (CO88, MNE = 132%; and CO99, MNE = 222%). Carefully considering the nature of the site (see Table 1), it becomes evident that CO13 would report much higher local [NH_3] due to its urban location in Fort Collins, CO and by being surrounded by agricultural land. CO88 and CO99 are in remote locations in the Rocky Mountain National Park. Although the sites are in proximity, there is significant difference in land use and altitude, which causes the observed differences. This exercise not only verifies that the long-term trend seen in the model is valid by matching empirical evidence, it also cautions against use of surface measurements as representative of regional concentrations due to the strong local effects on [NH_3].

3.2. Increasing Long-Term Trend of [NH_3]

One of the most noteworthy results is embodied in Figure 4, where the linear trend of model simulated surface layer ammonia over North America from 2001 to 2016 is presented. Delineation of the region into three on the basis of concentrations (Figure 2) becomes important. Figure 4 is virtually the inversion of Figure 2; in addition to the increasing trend in ammonia being East (~5 to 12%/year) > Central (~1 to 7%/year) > West (~0 to 5%/year), the ammonia hotspots appear to show a less increasing or decreasing trend. To visualize the long-term trends better and compare them with surface measurements, we normalize the annual averages of [NH_3] during the period of study with respect to the 2016 average (Figure 5) for both the model simulated and observed values at 13 AMoN sites that have data since 2008 (Table 1, site index 1–13) and three additional sites in the West that have measurements since 2010–2011 (A, B, and C). The corresponding linear regression slope, correlation coefficient (*r*), and *p* value for both observations and model simulations are given in Table 2. The long-term increase is evident for most of the selected sites, with average upward slope largest (smallest) and *p* value lowest (highest) in the East (West) based on both observations and model simulations. The increasing trend is statistically highly significant for most sites in the East (p value < 0.01)

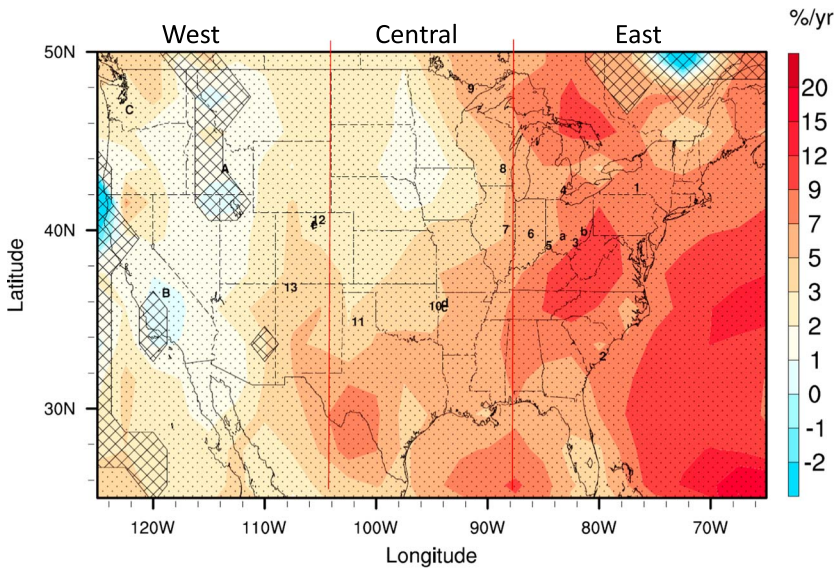

Figure 4. GEOS-Chem simulated linear trends of surface layer gas-phase NH_3 concentrations from 2001 to 2016. Color bar indicates values of the linear regression slope-percentage change in [NH_3] per year. Regions with the coefficient of the annual trend statistically different from zero at the 95% confidence level are stippled. Vertical blue line segments separate the North American region into West, Central, and East regions. The locations of AMoN sites in Table 1 are marked on the map with corresponding site index.

and significant for most sites in the middle (p value < 0.05). For the sites in the West, p values are generally larger than 0.1 during the periods of observations and thus the trends are statistically not significant. The model, in general, captures the increasing trend as well as the extent of increase, considering the likely bias due to coarse horizontal resolution of the model.

It can be seen from Figures 2 and 4 that the long-term ammonia trend is inversely related to [NH_3]. This is indicative of the significance of the emission/concentration regime and how the effect of chemistry varies in these regimes. We rule out the effect of ammonia emission change, which is very small during the period of study (see Figure 1). As we show in the next section, the long-term ammonia trend in the United States appears to be largely associated with reduction in SO_2 and NO_x emissions.

3.3. Sensitivity of [NH_3] to SO_2 and NO_x Emissions

The most significant reaction of ammonia in the atmosphere is its neutralization of acidic species—sulfuric acid (precursor is SO_2) and nitric acid (precursor is NO_x). This mainly determines the amount of ammonia that remains in the gas phase and the amount that becomes particulate NH_4^+. From 2001 to 2016, the U.S. SO_2 emissions reduce by a factor of 5–6 and NO_x emissions decrease by a factor 2–3 (see Figure 1). Here we examine quantitatively the effect of SO_2 as well as NO_x emissions on the concentration of ammonia (Figures 6 and 7). Figure 6 shows simulated model surface layer annual mean [NH_3] for 2016 and 2001 baseline cases, and sensitivity study cases for 2016 but with SO_2 emission only or both SO_2 and NO_x emissions replaced with that of 2001. The simulated domain average model surface layer [NH_3] for 2016 baseline case (Figure 6a) is 1.05 ppb, 67% higher that of 2001 baseline case (Figure 6b). Since NH_3 emission in 2016 is ~5% higher than that of 2001, most of the [NH_3] increase from 2001 to 2016 must be due to other factors such as changes in meteorology and emissions of SO_2 and NO_x (Sutton et al., 2003). Meteorology is known to have a strong influence on the inter-annual variability of [NH_3]—higher temperatures generally mean higher emission of ammonia, and wetter years mean more ammonia deposition, and the transport of ammonia and more importantly particulate ammonium determines the spatial distribution of [NH_3]. With SO_2 and NO_x emissions fixed at the 2001 levels, simulated domain mean [NH_3] for 2016 (Figure 6d) is 8% higher than that of the 2001 baseline case (Figure 6b), indicating that the meteorological difference is minor contribution (~8% − 5% = 3%) to the increase in [NH_3] over the United States. With only SO_2 emission fixed at the 2001 levels, model simulated domain mean [NH_3]

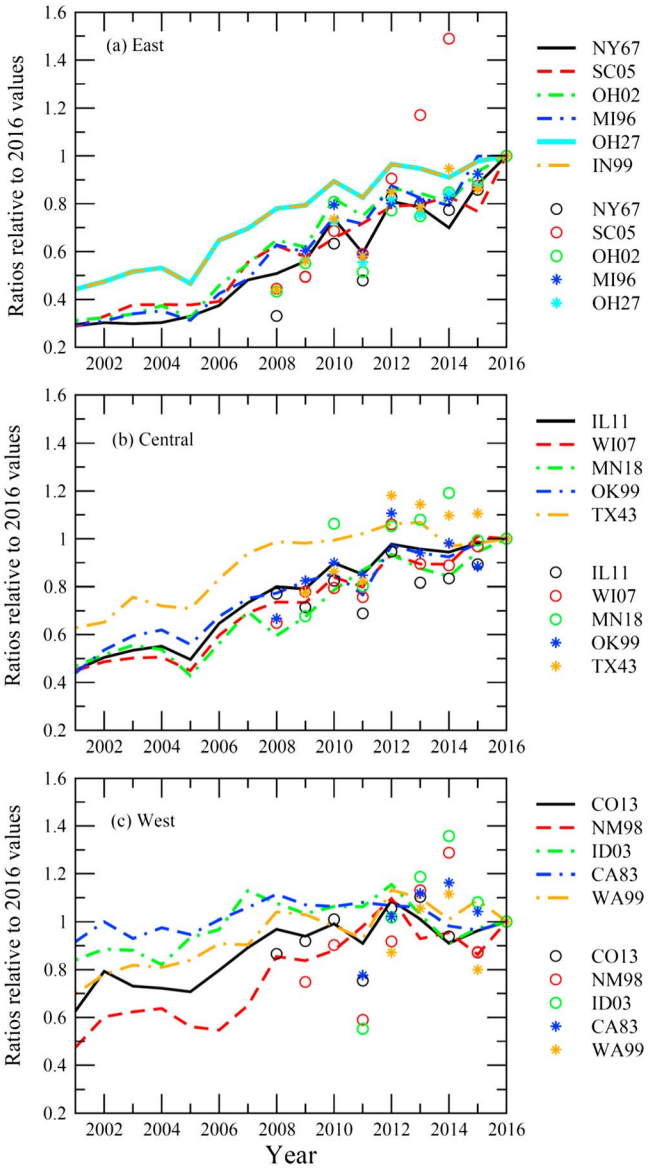

Figure 5. Long-term trend of $[NH_3]$ in selected AMoN sites in each region (top to bottom: East, Central, and West): Model simulations (lines) versus measurements (symbols). Values are normalized with the 2016 annual mean.

for 2016 (Figure 6c) is 0.8 ppb. It can be seen from the differences among $[NH_3]^{baseline}_{2016}$ (Figure 6a), $[NH_3]^{2001SO_2}_{2016}$ (Figure 6c), and (d) $[NH_3]^{2001SO_2\&NO_x}_{2016}$ (Figure 6d) that SO_2 contributes to about 2/3 and NO_x to 1/3 of the changes in $[NH_3]$ over the United States from 2001 to 2016.

The above analysis focused on averaged values over the domain of study. To illustrate further the spatial disparity, Figure 7 presents ratios of $[NH_3]^{baseline}_{2016}$ to $[NH_3]^{2001SO_2}_{2016}$, $[NH_3]^{baseline}_{2016}$ to $[NH_3]^{2001SO_2\&NO_x}_{2016}$, and $[NH_3]^{baseline}_{2001}$ to $[NH_3]^{2001SO_2\&NO_x}_{2016}$. These figures indicate that if emissions of (a) SO_2 only and (b) both SO_2 and NO_x remained unchanged over the 16-year period, current $[NH_3]$ over the United States would be significantly lower, by a factor of ~1.88 and ~2.25 (according to domain-averaged ratios), respectively. Figure 7c indicates the smaller role of meteorological and ammonia emission changes. These are in tune with our previous results indicative of SO_2 contributing to ~2/3 and NO_x to ~1/3 of the changes in $[NH_3]$. It becomes evident that the effect of SO_2 and NO_x are the most important in determining surface $[NH_3]$ trends over the United States in the last decade.

The spatial disparity, between Eastern and Western United States, in the ammonia trends (as shown in Figures 4 and 7) is posited to be due to the different NH_3 and SO_2 and NO_x (generally co-emitted pollutants) regimes. Eastern United States has the lowest average ammonia emissions in the United States, but the highest concentrations of SO_2 and NO_x. Although the percentage decrease in these acid precursor gases is assumed to be the same across continental United States in the present study, the absolute reduction is therefore greatest in the East. This explains the higher increasing trend of $[NH_3]$ over Eastern United States. Central United States has the highest ammonia emissions as well as lower absolute reductions in SO_2 and NO_x. Thus $[NH_3]$ is more dependent on emissions and not partitioning in this region, resulting in a lower increasing trend as compared to the East. Western United States has the lowest $[SO_2]$ and $[NO_x]$ and therefore the increasing trend in $[NH_3]$ is least in this region. The correspondence of the results of the acidic precursor gas sensitivity analysis (Figure 7) with the $[NH_3]$ spatiotemporal trend (Figure 4) rather than the absolute $[NH_3]$ (Figure 2) over the United States thus provides further credence to the importance of SO_2 and NO_x emissions in determining the increasing trend of $[NH_3]$ over the United States.

4. Summary and Discussion

This paper provides the first long-term study of surface ammonia trends over the United States using GEOS-Chem—a global 3-D tropospheric chemistry model. Results are validated by comparison of simulated $[NH_3]$ with observations made from the AMoN. Clear spatial differences are observed over the United States in the atmospheric ammonia concentration, which is highly dependent on the cropland distribution, that is, highly emission dependent. Eastern United States has the lowest and Central United States the highest surface $[NH_3]$. These features are captured well by the model. When examining the long-term trend from 2001 to 2016 in the model, the spatial differences are flipped, with Eastern United States showing the highest increasing trend in surface $[NH_3]$.

The claim that SO_2 and NO_x emission reductions have a role in determining ambient $[NH_3]$ is examined. With the reducing acid precursor gases owing to the stringent regulations in place after the Clean Air Act

Table 2
Linear regression slope, correlation coefficient (r), and p value for each individual measurement station shown in Figure 5 (both for the observations and the model calculations for the whole period [only model] and for the matching periods [model and observations])

	Observations (AMoN sites in Figure 5)				Model calculations (matching periods of obs.)				Model calculations (whole period)			
Site ID	# of year	slope	*r*	*p* value	# of year	slope	*r*	*p* value	# of year	slope	*r*	*p* value
NY67	9	0.073	0.919	0.0002	9	0.051	0.873	0.0011	16	0.047	0.957	0
SC05	9	0.092	0.746	0.0105	9	0.042	0.9	0.0005	16	0.044	0.971	0
OH02	9	0.06	0.868	0.0013	9	0.04	0.894	0.0006	16	0.05	0.969	0
MI96	8	0.049	0.856	0.0034	8	0.051	0.899	0.0013	16	0.051	0.971	0
OH27	8	0.055	0.88	0.0021	8	0.025	0.832	0.0052	16	0.041	0.963	0
IN99	9	0.063	0.91	0.0003	9	0.026	0.882	0.0009	16	0.041	0.963	0
IL11	9	0.027	0.715	0.0151	9	0.026	0.897	0.0006	16	0.04	0.966	0
WI07	9	0.038	0.795	0.0052	9	0.035	0.929	0.0001	16	0.041	0.97	0
MN18	8	0.037	0.549	0.0793	8	0.035	0.841	0.0045	16	0.037	0.937	0
OK99	9	0.029	0.648	0.0295	9	0.028	0.858	0.0016	16	0.036	0.964	0
TX43	8	0.042	0.659	0.0377	8	−0.001	−0.067	0.5625	16	0.028	0.874	0
CO13	9	0.01	0.254	0.2548	9	0.002	0.108	0.3912	16	0.023	0.839	0
NM98	8	0.047	0.53	0.0883	8	0.01	0.279	0.2519	16	0.035	0.878	0
ID03	6	0.074	0.514	0.1482	6	−0.028	−0.627	0.9084	16	0.011	0.524	0.0186
CA83	6	0.035	0.488	0.1631	6	−0.022	−0.852	0.9851	16	0.005	0.388	0.069
WA99	5	0	0.003	0.4979	5	−0.027	−0.739	0.9252	16	0.023	0.863	0

amendments in 1990, less ammonia is used up in their neutralization. Further, dry deposition is likely hindered due to less acidic surfaces for the ammonia to deposit onto. Ultimately, the decreasing trend of $[SO_2]$ and $[NO_x]$ results in an increasing trend in $[NH_3]$, the extent of which is not explained by the trend in its emission. In our study, we show that over the United States, the effects of meteorology are

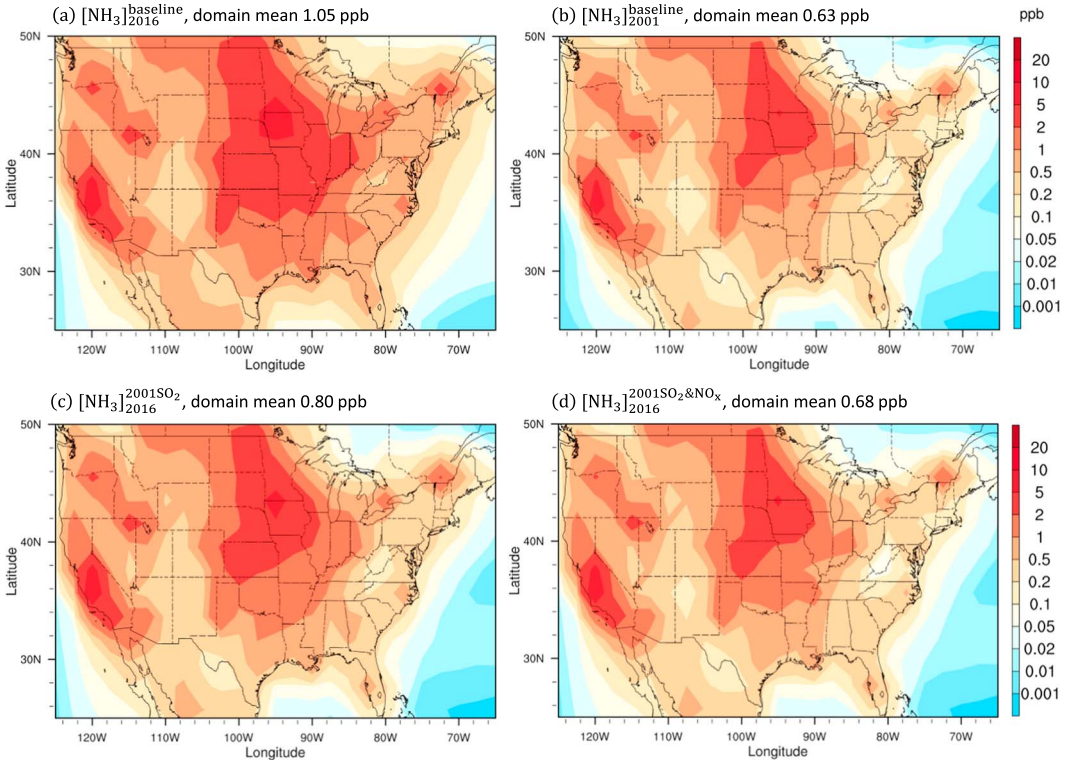

Figure 6. The effect of SO_2 and NO_x emissions on simulated annual mean $[NH_3]$ in the model surface layer over the United States: (a) 2016 baseline ($[NH_3]^{baseline}_{2016}$), (b) 2001 baseline ($[NH_3]^{baseline}_{2001}$), (c) 2016 with SO_2 emission of 2001 ($[NH_3]^{2001SO_2}_{2016}$), and (d) 2016 with both SO_2 and NO_x emissions of 2001 ($[NH_3]^{2001SO_2\&NO_x}_{2016}$). Mean values on each panel are domain mean $[NH_3]$ in ppb.

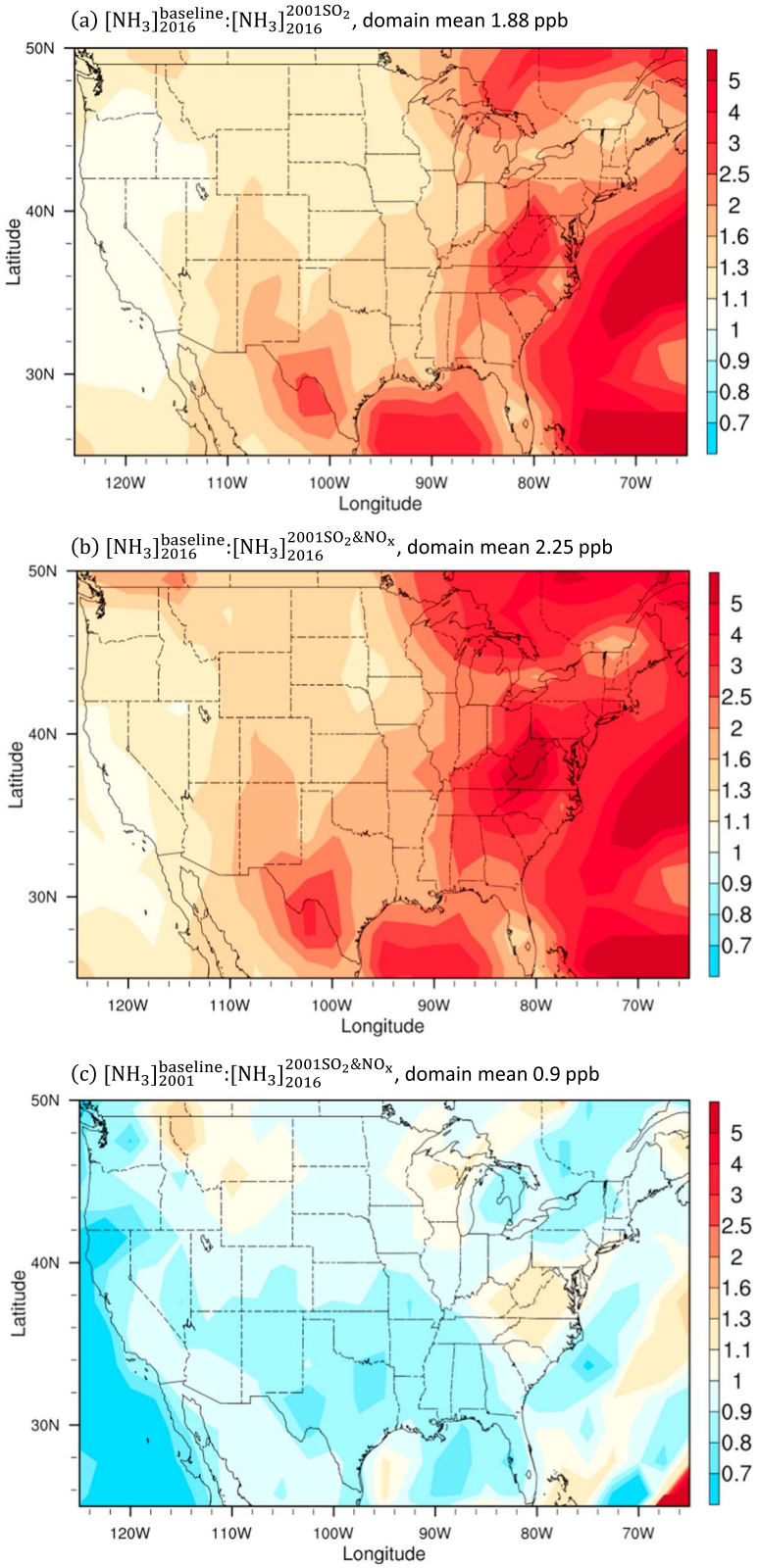

Figure 7. (a) Ratio of GEOS-Chem simulated 2016 average surface $[NH_3]$ with realistic emissions ($[NH_3]^{baseline}_{2016}$) to that with emission of SO_2 fixed at the year 2001 ($[NH_3]^{2001SO2}_{2016}$). (b) Ratio of $[NH_3]^{baseline}_{2016}$ to that with emission of both SO_2 and NO_x fixed at the year 2001 ($[NH_3]^{2001SO2\&NOx}_{2016}$). (c) Ratio of GEOS-Chem simulated 2001 average surface $[NH_3]$ with realistic emissions ($[NH_3]^{baseline}_{2001}$) to $[NH_3]^{2001SO2\&NOx}_{2016}$.

not significant in determining [NH_3] trends in the long-term. Considering various emission scenarios in the model indicates that changes in SO_2 contributes to around ~2/3 and NO_x to around ~1/3 of the observed increasing trend in ammonia over the United States from 2001 to 2016, where their emissions are reduced by a factor of 5–6 (SO_2) and 2–3 (NO_x). It should be noted that the possible effect of soil temperature long-term change on the surface layer NH_3 concentration (Warner et al., 2017) remains to be investigated. Further sensitivity study, probably taking into account recently developed ammonia bidirectional flux parameterization (Zhu et al., 2015), is needed.

The present study is limited by accuracy of the model in capturing the processes (emission, deposition, gas/particle partitioning) controlling ambient [NH_3]. An improvement in spatially heterogeneous long-term emission changes and more in-depth analysis and comparisons with additional observations (including both station and satellite based) may provide more compelling evidence of the key role of the acid precursor gases in determining [NH_3] trends over the United States. Examining the yearly averages as presented in the present work might have hidden interesting effects of diurnal and seasonal variations. However, as a first study examining long-term trends of ammonia over the United States through modeling, and with the verification of the effect of SO_2 and NO_x on trends in [NH_3], we hope this paper spurs more work in understanding the variability of ammonia, especially through modeling, given its demonstrated importance in the chemistry of the atmosphere and direct and indirect effects on particles in the atmosphere, radiative forcing changes, and impacts on the health of the ecosystem and human beings.

Acknowledgments

This study was supported by NASA under grant NNX13AK20G, NSF under grant 1550816, and NYSERDA under contract 100416. Ammonia Monitoring Network (AMoN) data are available from National Atmospheric Deposition Program (NRSP-3), 2017, NADP Program Office, Illinois State Water Survey, University of Illinois, Champaign, IL 61820 (http://nadp.sws.uiuc.edu/AMoN/). The GEOS-Chem model is managed by the Atmospheric Chemistry Modeling Group at Harvard University with support from NASA's Atmospheric Chemistry Modeling and Analysis Program. The work described in this paper is based on GEOS-Chem version 10-01. The GEOS-Chem model is a community model and can be downloaded from http://geos-chem.org/. The figures presented in this paper were generated using NCAR Command Language (NCL).

References

Alebic-Juretic, A. (2008). Airborne ammonia and ammonium within the Northern Adriatic area, Croatia. *Environmental Pollution*, *154*(3), 439–447. https://doi.org/10.1016/j.envpol.2007.11.029

Beem, K. B., Raja, S., Schwandner, F. M., Taylor, C., Lee, T., Sullivan, A. P., et al. (2010). Deposition of reactive nitrogen during the Rocky Mountain airborne nitrogen and sulfur (RoMANS) study. *Environmental Pollution*, *158*(3), 862–872. https://doi.org/10.1016/j.envpol.2009.09.023

Bey, I., Jacob, D. J., Yantosca, R. M., Logan, J. A., Field, B. D., Fiore, A. M., et al. (2001). Global modeling of tropospheric chemistry with assimilated meteorology: Model description and evaluation. *Journal of Geophysical Research*, *106*(D19), 23,073–23,095. https://doi.org/10.1029/2001jd000807

Butler, T., Vermeylen, F., Lehmann, C. M., Likens, G. E., & Puchalski, M. (2016). Increasing ammonia concentration trends in large regions of the USA derived from the NADP/AMoN network. *Atmospheric Environment*, *146*, 132–140. https://doi.org/10.1016/j.atmosenv.2016.06.033

EEA (2017). *European Environment Agency, Annual European Union (EU) LRTAP Convention emission inventory report 1990–2015*. Luxembourg: Publications Office of the European Union.

Ellis, R. A., Jacob, D. J., Sulprizio, M. P., Zhang, L., Holmes, C. D., Schichtel, B. A., et al. (2013). Present and future nitrogen deposition to national parks in the United States: Critical load exceedances. *Atmospheric Chemistry and Physics*, *13*(17), 9083–9095. https://doi.org/10.5194/acp-13-9083-2013

Erisman, J. W., Bleeker, A., Galloway, J., & Sutton, M. S. (2007). Reduced nitrogen in ecology and the environment. *Environmental Pollution*, *150*(1), 140–149. https://doi.org/10.1016/j.envpol.2007.06.033

Evans, M. J., & Jacob, D. J. (2005). Impact of new laboratory studies of N_2O_5 hydrolysis on global model budgets of tropospheric nitrogen oxides, ozone, and OH. *Geophysical Research Letters*, *32*, L09813. https://doi.org/10.1029/2005gl022469

Fangmeier, A., Hadwiger-Fangmeier, A., Van der Eerden, L., & Jäger, H.-J. (1994). Effects of atmospheric ammonia on vegetation—A review. *Environmental Pollution, 86*(1), 43–82. https://doi.org/10.1016/0269-7491 (94)90008-6

Ferm, M., & Hellsten, S. (2012). Trends in atmospheric ammonia and particulate ammonium concentrations in Sweden and its causes. *Atmospheric Environment*, *61*, 30–39. https://doi.org/10.1016/j.atmosenv.2012.07.010

Fountoukis, C., & Nenes, A. (2007). ISORROPIA II: A computationally efficient thermodynamic equilibrium model for K^+–Ca^{2+}–Mg^{2+}–NH_4^+–Na^+–SO_4^{2-}–NO_3^-–Cl^-–H_2O aerosols. *Atmospheric Chemistry and Physics*, *7*(17), 4639–4659. https://doi.org/10.5194/acp-7-4639-2007

Giglio, L., Randerson, J. T., & van der Werf, G. R. (2013). Analysis of daily, monthly, and annual burned area using the fourth-generation global fire emissions database (GFED4). *Journal of Geophysical Research: Biogeosciences*, *118*, 317–328. https://doi.org/10.1002/jgrg.20042

Guenther, A. B., Jiang, X., Heald, C. L., Sakulyanontvittaya, T., Duhl, T., Emmons, L. K., & Wang, X. (2012). The model of emissions of gases and aerosols from nature version 2.1 (MEGAN2.1): An extended and updated framework for modeling biogenic emissions. *Geoscientific Model Development*, *5*(6), 1471–1492. https://doi.org/10.5194/gmd-5-1471-2012

Heald, C. L., Collett, J. L. Jr., Lee, T., Benedict, K. B., Schwandner, F. M., Li, Y., et al. (2012). Atmospheric ammonia and particulate inorganic nitrogen over the United States. *Atmospheric Chemistry and Physics*, *12*(21), 10,295–10,312. https://doi.org/10.5194/acp-12-10295-2012

Horvath, L., Fagerli, H., & Sutton, M. A. (2009). Long-term record (1981–2005) of ammonia and ammonium concentrations at K-Puszta Hungary and the effect of sulphur dioxide emission change on measured and modelled concentrations. In M. A. Sutton, S. Reis, & S. M. Baker (Eds.), *Atmospheric Ammonia* (pp. 181–185). Dordrecht, Netherlands: Springer.

Hu, Q., Zhang, L., Evans, G. J., & Yao, X. (2014). Variability of atmospheric ammonia related to potential emission sources in downtown Toronto, Canada. *Atmospheric Environment*, *99*, 365–373. https://doi.org/10.1016/j.atmosenv.2014.10.006

Keller, C. A., Long, M. S., Yantosca, R. M., Da Silva, A. M., Pawson, S., & Jacob, D. J. (2014). HEMCO v1.0: A versatile, ESMF-compliant component for calculating emissions in atmospheric models. *Geoscientific Model Development*, *7*(4), 1409–1417. https://doi.org/10.5194/gmd-7-1409-2014

Kirkby, J., Curtius, J., Almeida, J., Dunne, E., Duplissy, J., Ehrhart, S., et al. (2011). Role of sulphuric acid, ammonia and galactic cosmic rays in atmospheric aerosol nucleation. *Nature*, *476*(7361), 429–433. https://doi.org/10.1038/nature10343

Li, Y., Thompson, T. M., van Damme, M., Chen, X., Benedict, K. B., Shao, Y., et al. (2017). Temporal and spatial variability of ammonia in urban and agricultural regions of northern Colorado, United States. *Atmospheric Chemistry and Physics*, *17*(10), 6197–6213. https://doi.org/10.5194/acp-17-6197-2017

Martin, R. V., Jacob, D. J., Yantosca, R. M., Chin, M., & Ginoux, P. (2003). Global and regional decreases in tropospheric oxidants from photochemical effects of aerosols. *Journal of Geophysical Research*, *108*(D3), 4097. https://doi.org/10.1029/2002jd002622

Murray, L. T., Jacob, D. J., Logan, J. A., Hudman, R. C., & Koshak, W. J. (2012). Optimized regional and interannual variability of lightning in a global chemical transport model constrained by LIS/OTD satellite data. *Journal of Geophysical Research*, *117*, D20307. https://doi.org/10.1029/2012jd017934

NADP (2017). Ammonia Monitoring Network (AMoN), National Atmospheric Deposition Program (NRSP-3). 2017. NADP Program Office, Illinois State Water Survey, University of Illinois, Champaign, IL 61820. Available from http://nadp.sws.uiuc.edu/AMoN/

Park, R. J., Jacob, D. J., Field, B. D., Yantosca, R. M., & Chin, M. (2004). Natural and transboundary pollution influences on sulfate-nitrate-ammonium aerosols in the United States: Implications for policy. *Journal of Geophysical Research*, *109*, D15204. https://doi.org/10.1029/2003jd004473

Paulot, F., Jacob, D. J., Pinder, R. W., Bash, J. O., Travis, K., & Henze, D. K. (2014). Ammonia emissions in the United States, European Union, and China derived by high-resolution inversion of ammonium wet deposition data: Interpretation with a new agricultural emissions inventory (MASAGE_NH3). *Journal of Geophysical Research: Atmospheres*, *119*, 4343–4364. https://doi.org/10.1002/2013jd021130

Pye, H. O. T., & Seinfeld, J. H. (2010). A global perspective on aerosol from low-volatility organic compounds. *Atmospheric Chemistry and Physics*, *10*(9), 4377–4401. https://doi.org/10.5194/acp-10-4377-2010

Schiferl, L. D., Heald, C. L., van Damme, M., Clarisse, L., Clerbaux, C., Coheur, P.-F., et al. (2016). Interannual variability of ammonia concentrations over the United States: Sources and implications. *Atmospheric Chemistry and Physics*, *16*(18), 12,305–12,328. https://doi.org/10.5194/acp-16-12305-2016

Sutton, M. A., Asman, W. A., Ellermann, T., Van Jaarsveld, J. A., Acker, K., Aneja, V., et al. (2003). Establishing the link between ammonia emission control and measurements of reduced nitrogen concentrations and deposition. *Environmental Monitoring and Assessment*, *82*(2), 149–185.

Tang, Y. S., Braban, C. F., Dragosits, U., Dore, A. J., Simmons, I., van Dijk, N., et al. (2018). Drivers for spatial, temporal and long-term trends in atmospheric ammonia and ammonium in the UK. *Atmospheric Chemistry and Physics*, *18*(2), 705–733. https://doi.org/10.5194/acp-18-705-2018

Tang, Y. S., Dragosits, U., van Dijk, N., Love, L., Simmons, I., & Sutton, M. A. (2009). Assessment of Ammonia and ammonium trends and relationship to critical levels in the UK National Ammonia Monitoring Network (NAMN). *Atmospheric Ammonia*, 187–194. https://doi.org/10.1007/978-1-4020-9121-6_13

USDA-NASS (2017). United States Department of Agriculture National Agricultural Statistics Service. Published crop-specific data layer [Online]. Available from: https://nassgeodata.gmu.edu/CropScape/ (accessed 10/28/2017; verified 10/28/2017).

van Damme, M., Wichink Kruit, R. J., Schaap, M., Clarisse, L., Clerbaux, C., Coheur, P. F., et al. (2014). Evaluating 4 years of atmospheric ammonia (NH3) over Europe using IASI satellite observations and LOTOS-EUROS model results. *Journal of Geophysical Research: Atmospheres*, *119*, 9549–9566. https://doi.org/10.1002/2014JD021911

van Donkelaar, A., Martin, R. V., Leaitch, W. R., Macdonald, A. M., Walker, T. W., Streets, D. G., et al. (2008). Analysis of aircraft and satellite measurements from the Intercontinental Chemical Transport Experiment (INTEX-B) to quantify long-range transport of east Asian sulfur to Canada. *Atmospheric Chemistry and Physics*, *8*(11), 2999–3014. https://doi.org/10.5194/acp-8-2999-2008

van Zanten, M. C., Wichink Kruit, R. J., Hoogerbrugge, R., Van der Swaluw, E., & van Pul, W. A. J. (2017). Trends in ammonia measurements in the Netherlands over the period 1993–2014. *Atmospheric Environment*, *148*, 352–360. https://doi.org/10.1016/j.atmosenv.2016.11.007

Warner, J. X., Dickerson, R. R., Wei, Z., Strow, L. L., Wang, Y., & Liang, Q. (2017). Increased atmospheric ammonia over the world's major agricultural areas detected from space. *Geophysical Research Letters*, *44*, 2875–2884. https://doi.org/10.1002/2016gl072305

Warner, J. X., Wei, Z., Strow, L. L., Dickerson, R. R., & Nowak, J. B. (2016). The global tropospheric ammonia distribution as seen in the 13-year AIRS measurement record. *Atmospheric Chemistry and Physics*, *16*(8), 5467–5479. https://doi.org/10.5194/acp-16-5467-2016

Wichink Kruit, R. J., Aben, J., de Vries, W., Sauter, F., van der Swaluw, E., van Zanten, M. C., & van Pul, W. A. J. (2017). Modelling trends in ammonia in the Netherlands over the period 1990–2014. *Atmospheric Environment*, *154*, 20–30. https://doi.org/10.1016/j.atmosenv.2017.01.031

Yao, X., & Zhang, L. (2016). Trends in atmospheric ammonia at urban, rural, and remote sites across North America. *Atmospheric Chemistry and Physics*, *16*(17), 11,465–11,475. https://doi.org/10.5194/acp-16-11465-2016

Yu, F. (2011). A secondary organic aerosol formation model considering successive oxidation aging and kinetic condensation of organic compounds: Global scale implications. *Atmospheric Chemistry and Physics*, *11*(3), 1083–1099. https://doi.org/10.5194/acp-11-1083-2011

Yu, F., & Luo, G. (2009). Simulation of particle size distribution with a global aerosol model: Contribution of nucleation to aerosol and CCN number concentrations. *Atmospheric Chemistry and Physics*, *9*(20), 7691–7710. https://doi.org/10.5194/acp-9-7691-2009

Zhang, L., Jacob, D. J., Knipping, E. M., Kumar, N., Munger, J. W., Carouge, C. C., et al. (2012). Nitrogen deposition to the United States: Distribution, sources, and processes. *Atmospheric Chemistry and Physics*, *12*(10), 4539–4554. https://doi.org/10.5194/acp-12-4539-2012

Zhu, L., Henze, D., Bash, J., Jeong, G.-R., Cady-Pereira, K., Shephard, M., et al. (2015). Global evaluation of ammonia bidirectional exchange and livestock diurnal variation schemes. *Atmospheric Chemistry and Physics*, *15*(22), 12,823–12,843. https://doi.org/10.5194/acp-15-12823-2015